MOLECULAR AND CELLULAR BIOLOGY, Oct. 2006, p. 7561–7574 Vol. 26, No. 20
0270-7306/06/$08.00+0 doi:10.1128/MCB.00605-06

Peroxisome Proliferator-Activated Receptor γ Regulates E-Cadherin Expression and Inhibits Growth and Invasion of Prostate Cancer‡

Jean-Sébastien Annicotte,[1] Irena Iankova,[1]† Stéphanie Miard,[1]† Vanessa Fritz,[2] David Sarruf,[1] Anna Abella,[1] Marie-Laurence Berthe,[3] Danièle Noël,[2] Arnaud Pillon,[1] François Iborra,[3] Pierre Dubus,[4] Thierry Maudelonde,[3] Stéphane Culine,[1] and Lluis Fajas[1,3]*

INSERM, U540, Equipe Avenir, Montpellier F-34090, France[1]; INSERM, U475, Montpellier F-34090, France[2]; Centre Hospitalier Universitaire Arnaud de Villeneuve, Laboratoire de Biologie Cellulaire, Montpellier F-34090, France[3]; and Université Victor Ségalen, EA2406 Histologie et Pathologie Moléculaire, Bordeaux F-33076, France[4]

Received 7 April 2006/Returned for modification 10 May 2006/Accepted 21 July 2006

Peroxisome proliferator-activated receptor γ (PPARγ) might not be permissive to ligand activation in prostate cancer cells. Association of PPARγ with repressing factors or posttranslational modifications in PPARγ protein could explain the lack of effect of PPARγ ligands in a recent randomized clinical trial. Using cells and prostate cancer xenograft mouse models, we demonstrate in this study that a combination treatment using the PPARγ agonist pioglitazone and the histone deacetylase inhibitor valproic acid is more efficient at inhibiting prostate tumor growth than each individual therapy. We show that the combination treatment impairs the bone-invasive potential of prostate cancer cells in mice. In addition, we demonstrate that expression of E-cadherin, a protein involved in the control of cell migration and invasion, is highly up-regulated in the presence of valproic acid and pioglitazone. We show that E-cadherin expression responds only to the combination treatment and not to single PPARγ agonists, defining a new class of PPARγ target genes. These results open up new therapeutic perspectives in the treatment of prostate cancer.

Prostate cancer is the most common form of cancer in men and the second leading cause of cancer deaths. Tumor growth is originally androgen dependent. Androgens exert their effects through activation of the androgen receptor (AR), a member of the hormone nuclear receptor superfamily. In the mature prostatic gland, the AR regulates the expression of genes involved in cell division and proliferation of the epithelial cells (26). The AR is also involved in several other aspects of prostate cellular metabolism, including lipid biosynthesis, and controls the production of specialized secretory proteins with prostate-restricted expression, such as prostate-specific antigen (PSA) (26). When prostate cancer is still hormone dependent, androgen ablation therapy causes regression of the tumor (18), likely through inactivation of the transcription of the AR target genes. However, the durability of this response is inadequate and many men develop recurrent androgen-independent prostate cancer, which has a very poor prognosis (see reference 11 for a review). Other nuclear receptors or locally produced factors that interact with nuclear receptors are likely involved in cell proliferation, differentiation, and apoptosis in the prostate. The peroxisome proliferator-activated receptor γ (PPARγ) is one such factor. PPARγ is another member of the hormone nuclear receptor superfamily. As for most of the other members of this family, its activity is regulated by ligands. Prostaglandin J2 and the antidiabetic drugs thiazolidinediones have been determined to be natural and synthetic ligands of PPARγ, respectively (for a review, see reference 9). PPARγ is highly expressed in the adipose tissue and is required for its development through regulation of the expression of adipocyte-specific genes, such as lipoprotein lipase or the fatty acid transport protein aP2. PPARγ is expressed in several other tissues in addition to adipose tissue, including gut, macrophages, lung, bladder, breast, and prostate, although its function in these tissues remains to be elucidated. Interestingly, PPARγ has been shown to be overexpressed in prostate cancer (15). Whereas the physiological function of PPARγ in normal epithelial cells is largely unknown, PPARγ activation was reported to inhibit the proliferation of prostate carcinoma cells (4, 21, 25, 34) and also other cancer lineages (7). These observations suggest that induction of differentiation by activation of PPARγ may represent a promising novel therapeutic approach for cancer, as already demonstrated with xenograft models of prostate (21). In addition, treatment of patients with advanced prostate cancer with the PPARγ agonist troglitazone resulted in the stabilization of prostate-specific antigen levels (25). In contrast, in a large-scale, placebo-controlled, randomized clinical trial, no effects on the PSA doubling time of prostate cancer patients were observed (35). These results suggest that PPARγ is not permissive for activation by ligands in these prostate cancer patients. One interesting hypothesis is that some factors could prevent activation of PPARγ by its ligands in cancer cells. One such factor is histone deacetylases (HDAC). Deacetylation of histones has been correlated with a transcriptionally silent state of chromatin. Inhibition of HDAC activity by natural or synthetic compounds results in the reversion of the phenotype of tumoral cells into normal cells or apoptosis of cancer cells (22). Although the precise mechanisms have not yet been elucidated, HDAC inhibition results

* Corresponding author. Mailing address: Equipe Avenir, INSERM U540, 60 rue de Navacelles, F-34090 Montpellier, France. Phone: 0033 467 043 082. Fax: 0033 467 540 598. E-mail: fajas@montp.inserm.fr.

† These authors contributed equally to this work.

‡ Supplemental material for this article may be found at http://mcb.asm.org/.

in the selective induction of endogenous genes that play roles in either differentiation or cell cycle arrest. We demonstrated in previous studies that HDAC3 is complexed with PPARγ in the promoters of PPARγ target genes and that this association results in the repression of these target genes. HDAC inhibitors, such as valproic acid or sodium butyrate (NaBu), had a synergistic effect with thiazolidinediones in the activation of PPARγ target genes (8). Therefore, HDAC inhibition could render PPARγ permissive to activation by its ligands. We show in this study that a combination treatment of HDAC inhibitors and PPARγ agonists results in the arrest of proliferation, increases apoptosis, and decreases the invasion potential of prostate cancer cells both in vitro and in vivo. Furthermore, we show that PPARγ agonists increase the expression of E-cadherin mRNA only in the presence of HDAC inhibitors, which defines a new class of PPARγ target genes.

MATERIALS AND METHODS

Materials and oligonucleotides. Pioglitazone was a kind gift of Takeda Pharmaceutical Industries (Osaka, Japan). Rosiglitazone was purchased from VWR-Calbiochem (Fontenay sous Bois, France). All chemicals, except if stated otherwise, were purchased from Sigma (St. Louis, MO). Anti-cyclin-dependent kinase 4 (anti-CDK4) (C-22), anti-PPARγ (H-100 for chromatin immunoprecipitation [ChIP] or N-20 for immunohistochemistry [IHC]), anti-HDAC3 (H-99), and anti-PCNA (PC-10) antibodies were from Santa Cruz Biotechnology (Santa Cruz, CA); anti-acetyl H4 (Lys 12) and anti-phospho-retinoblastoma (anti-^{P}pRb) (Ser 807/811) were from Cell Signaling (Beverly, MA); anti-p21 (Ab-1) was from EMD Biosciences (Darmstadt, Germany); anti-p27 was from NeoMarkers (Fremont, CA); and antibromodeoxyuridine (anti-BrdU) and anti-E-cadherin (NCH-38) antibodies were from DAKO (Glostrup, Denmark). The oligonucleotide sequences used for various experiments described in the manuscript are available upon request.

Cell culture, transient transfections, and siRNA. The LNCaP, DU145, PC3, and luminescent PC3 (30) prostate cancer cell lines were derived from stocks routinely maintained in the laboratory. Monolayer cell cultures were grown in Ham's F-12 medium supplemented with 10% fetal calf serum (FCS) (Invitrogen, Cergy-Pontoise, France). In all experiments, cells were treated for 48 h with the vehicle dimethyl sulfoxide (dilution, 1:2,000), 5×10^{-6} M pioglitazone, 5×10^{-6} M rosiglitazone, valproic acid (1.5 mM for PC3 cells, 0.75 mM for DU145 cells, and 0.375 mM for LNCaP cells), or both pioglitazone and valproic acid. Transient transfections were performed as described previously (2), and luciferase activity measurements were normalized for β-galactosidase activity to correct for differences in transfection efficiency. Graph values represent the means of three independent experiments. For small interfering RNA (siRNA) experiments, smart-pool siRNAs against HDAC3 (Dharmacon, Lafayette, CO) were transfected in PC3 cells by using DharmaFECT 2 (Dharmacon) according to the manufacturer's instructions. After 24 h, cells were treated as described above and incubated for 24 h. Effects of the siRNA on HDAC3 mRNA and protein levels are illustrated below (see Fig. 7B and C, respectively).

Apoptosis and BrdU assays, flow cytometry analysis, and phospho-pRb detection. Proliferating LNCaP, DU145, and PC3 cells were incubated for 48 h with the different treatments as described above. For all immunofluorescence experiments, cells were grown on coverslips. Apoptotic cells were detected using Alexa 568-conjugated annexin V labeling according to the manufacturer's instructions (Roche, Basel, Switzerland). For BrdU incorporation, cells were incubated for 4 h (PC3 and DU145 cells) or for 16 h (LNCaP cells) in the presence of 100 μM BrdU, harvested, and fixed with methanol. An additional treatment of the cells with 1.5 N HCl for 10 min was performed. Cells were then incubated with the anti-BrdU antibody (dilution, 1:100) for 16 h at 4°C, and BrdU staining was revealed using a Texas Red-conjugated anti-mouse immunoglobulin G (IgG). For phospho-pRb (^{P}pRb) immunofluorescence detection, PC3 cells were harvested after 48 h of treatment, fixed in methanol for 10 min at 4°C, and incubated for 16 h at 4°C with the anti-phospho-pRb antibody (dilution, 1:50), and phospho-pRb staining was revealed using a Texas Red-conjugated anti-rabbit IgG. At least 500 cells were counted. For fluorescence-activated cell sorter analysis, cells were harvested, fixed with 70% ethyl alcohol, and DNA was labeled with propidium iodide. Cells were sorted by fluorescence-activated cell sorter analysis (Coulter Electronics, Hialeah, FL), and cell cycle profiles were determined using ModFit software (Becton Dickinson, San Diego, CA).

RNA extraction, RT-PCR, and Q-PCR. RNA extraction and reverse transcription-PCR (RT-PCR) were performed as described previously (3). Quantitative PCR (Q-PCR) was carried out using a LightCycler and DNA double-strand-specific SYBR green I dye for detection (Roche). Q-PCR was performed using gene-specific oligonucleotides, and results were then normalized to RS9 levels.

Protein extracts and Western blot analysis. Preparation of protein extracts and sodium dodecyl sulfate-polyacrylamide gel electrophoresis, electrotransfer, and immunoblotting were performed as described previously (31).

Kinase assays. CDK4 immunoprecipitation and kinase assays were performed exactly as previously described (1).

In vivo murine models of prostate cancer. Male Rj:NMRI-nu (nu/nu) (Janvier, Le Genest-St-Isle, France) and CD17-SCID/bg (Harlan, Gannat, France) mice were maintained according to European Union guidelines for use of laboratory animals. In vivo experiments were performed in compliance with the French guidelines for experimental animal studies (agreement no. B-34-172-27). For in vivo proliferation studies, 3×10^6 luminescent PC3 cells were laterally injected subcutaneously in nude mice at 6 weeks of age. Five days after subcutaneous injection, cohorts (10 mice/group) were orally administrated vehicle (0.5% carboxymethyl cellulose [CMC]), pioglitazone (30 mg/kg of body weight/day in 0.5% CMC), valproic acid (150 mg/kg/day in 0.5% CMC), or both compounds for a period of 4 weeks. Tumor progression was determined by measuring the volume of the tumor with a caliper. Tumor tissues were collected, weighed, fixed in 4% phosphate-buffered formalin, and embedded in paraffin for immunohistological analyses. For in vivo bone invasion studies, subconfluent monolayers of luminescent PC3 cells were detached by trypsinization, washed, and resuspended in phosphate-buffered saline to the working concentration of 5×10^5 cells/10 μl. All tibia injections were performed on SCID mice (10 mice/group) anesthetized with pentobarbital (50 mg/kg). The proximal end of the left tibial bones was exposed surgically in a flex position, and 10 μl of phosphate-buffered saline containing tumor cells was injected into the bone marrow space with a 26-gauge needle. Mice were treated 7 days after intratibial injection with vehicle (0.5% CMC), pioglitazone (30 mg/kg/day in 0.5% CMC), valproic acid (300 mg/kg/day in 0.5% CMC), or both compounds for a period of 4 weeks and monitored weekly for tumor growth kinetic by use of bioluminescence imaging with a NightOWL LB981 charge-coupled-device camera (Berthold Technologies, Bad Wildbad, Germany) and WinLight software (Berthold Technologies). Left and right legs were harvested and fixed in 4% phosphate-buffered formalin, X rays of the legs were taken, and invasion potential was scored by four blind comparisons of X-ray radiographs. Scores ranged from 0 (no invasion) to 4 (high degree of invasion). For both xenograft mouse models, tumor formation was verified by use of bioluminescence imaging 1 day before starting treatment. No failure rate for tumor initiation was observed, and tumor growth occurred at the same rate.

IHC and histology. IHC was performed as described previously (2). Briefly, after antigen retrieval, 5 μm formalin-fixed luminescent PC3 tumor sections was incubated with the anti-PCNA (dilution, 1:500), anti-p21 (dilution, 1:20), and anti-E-cadherin (dilution, 1:25) antibodies, and a LandMark prostate tissue microarray (Ambion, Austin, TX) containing 5 μm formalin-fixed, paraffin-embedded human normal and tumor prostate sections was incubated with the anti-PPARγ (dilution, 1:25) or the anti-acetyl H4 (dilution, 1:25) antibody. Immunostaining was revealed using peroxidase-conjugated anti-mouse (for PCNA, p21, and E-cadherin; Jackson Immunoresearch, Cambridgeshire, United Kingdom), anti-goat (for PPARγ; Jackson Immunoresearch), or anti-rabbit (for acetylated H4 [AcH4]; Jackson Immunoresearch) secondary antibody and diaminobenzidine chromogen (DAKO) as a substrate. Sections were counterstained with hematoxylin. For E-cadherin, immunofluorescence staining was revealed using a Texas Red-conjugated anti-mouse secondary antibody. Negative-control experiments using mouse, rabbit, or goat IgG were performed, and no staining was observed under these conditions. Trained pathologists analyzed the PPARγ, acetyl H4, and E-cadherin staining. Immunohistochemical quantification was based on two parameters, the intensity of the staining and the percentage of cells positively stained, leading to 4 groups: 0, no staining; 1, weak positive staining; 2, moderate staining; and 3, strong staining.

Invasion assay. A Boyden chamber migration assay was performed as described previously (12). Briefly, polycarbonate filters (12 μm pore size) were coated with 60 μg of Matrigel (Becton Dickinson). Cells were harvested in medium containing 3% FCS and ligands (vehicle, 5 μM pioglitazone, 1.5 mM valproic acid, or both compounds) and added to the top chamber (1×10^6 cells per chamber). Medium supplemented with 10% FCS and ligands was used in the bottom compartment as a chemoattractant. To correct for proliferation and/or cell death due to our treatments, cells were cultured in parallel in 12-well plates in medium containing 3% FCS and ligands (control plate corresponding to total

cells). Chambers and plates were incubated for 48 h at 37°C, and cells that had traversed the Matrigel and spread on the bottom surface of the filter as well as cells from control plates were then quantified using 3(4,5-dimethyl-thiazol-2-yl)2,5-diphenol tetrazolium bromide and determination of optical density at 540 nm. Experiments were performed in triplicate, and results are expressed as percentages of invading cells relative to percentages of total control cells.

EMSA. Electromobility shift assays (EMSA) were performed as described previously (2, 10). Briefly, in vitro-translated PPARγ and retinoid X receptor α (RXRα) were incubated for 15 min at 21°C in a total volume of 20 μl binding buffer [10 mM Tris-HCl (pH 7.9), 40 mM KCl, 10% glycerol, 0.05% Nonidet P-40, 1 mM dithiothreitol, and 1 μg poly(dI:dC)] in the presence of 2 ng of a T4 polynucleotide kinase end-labeled, double-stranded oligonucleotide probe. For gel supershift assays, 2 μg of IgG or PPARγ antibody was added to the reaction mixture. DNA-protein complexes were separated by electrophoresis on a 4% polyacrylamide gel in 0.25% Tris-borate-EDTA at 4°C and 10 V/cm.

Cloning of the E-cadherin and aP2 promoters. The E-cadherin and aP2 promoters were cloned using BD Advantage GC genomic polymerase mix (BD Biosciences Clontech, Palo Alto, CA) and genomic DNA as a template. PCR amplifications were performed according to the manufacturer's instructions and cloned in the pGL3-basic vector (Promega Life Science, Madison, WI). An E-cadherin promoter deletion mutant devoid of the PPARγ response element (PPRE) was obtained by PCR using specific primers and cloned as described above. The different pGL3 promoter constructs were sequenced and used in transient transfections.

Coimmunoprecipitation. Immunoprecipitation assays were performed as previously described (8).

ChIP and Re-ChIP. ChIP assays were performed as described previously (3). Chromatin reimmunoprecipitation (Re-ChIP) assays were performed as described previously (23). Briefly, proteins from PC3 cells treated for 48 h with different ligands were formaldehyde cross-linked to DNA. After lysis and DNA sonication, proteins were immunoprecipitated using an anti-PPARγ antibody. After being washed, DNA-protein complexes were eluted in 10 mM dithiothreitol for 30 min at 37°C and reimmunoprecipitated using IgG (negative control) or anti-HDAC3 antibody. Cross-linking was then reversed by heating the samples at 65°C for 16 h. DNA was then purified using a QIAGEN PCR purification kit (QIAGEN, Courtabœuf, France), and PCR amplification was performed using promoter-specific oligonucleotide primers.

Statistical analysis. Data are presented as means ± standard errors of the means, except for tumor measurements (volume and mass), which are presented as medians. Group means and medians were compared by factorial analysis of variance. Upon determination of significant interactions, differences between individual group means and medians were analyzed by Fisher's protected least-squares difference test. Differences were considered statistically significant at P of <0.05.

RESULTS

Synergistic action of PPARγ agonists and HDAC inhibitors in the control of cell proliferation and apoptosis in prostate cancer cells. We have demonstrated previously that HDAC inhibitors have a synergistic action with PPARγ agonists in the activation of PPARγ target genes and adipocyte differentiation (8). Since both PPARγ agonists and HDAC inhibitors independently arrest proliferation of prostate cancer cells, we wanted to test the synergy of both agents in the control of prostate cancer cell growth. BrdU incorporation studies with the androgen-dependent LNCaP (AR mutant, Rb wild type [wt], p53 wt) cell line indicated that percentages of BrdU-positive cells were significantly decreased upon 48 h of pioglitazone and rosiglitazone treatments compared to percentages of control cells (with LNCap, 33.8% ± 0.1% for vehicle-treated cells, 26.8% ± 1.4% for pioglitazone-treated cells, and 27.5% ± 2.5% for rosiglitazone-treated cells) (Fig. 1A). Moreover, a significant decrease in BrdU incorporation was observed when cells were incubated in the presence of the HDAC inhibitor valproic acid (33.8% ± 0.1% for vehicle-treated cells versus 4.8% ± 0.8% for valproic acid-treated cells) (Fig. 1A). Most interestingly, the combination treatment of pioglitazone plus valproic acid or rosiglitazone plus valproic acid decreased the proliferation index to 1.5% ± 0.1% or 1.6% ± 0.01%, respectively. To further prove that the effect of the combination treatment was independent of the cell line, two androgen-independent prostate cancer cell lines, i.e., DU145 (AR^-, Rb^-, p53 mutant) and PC3 (AR^-, Rb wt, $p53^-$) cells, were subjected to BrdU incorporation (Fig. 1B and C). With DU145 cells, PPARγ agonists and valproic acid alone demonstrated no inhibitory effect on proliferation (Fig. 1B), whereas with PC3 cells, a single valproic acid treatment resulted in a decreased proliferation index (12.6% ± 2.1% for vehicle-treated cells versus 6.9% ± 1.6% for valproic acid-treated cells) (Fig. 1C). Importantly, as observed for LNCaP cells, moderate and strong inhibitory effects on proliferation were obtained when using the combination of PPARγ agonists and valproic acid with DU145 cells (33.9% ± 4.5% for vehicle-treated cells versus 24.3% ± 1.8% for pioglitazone plus valproic acid-treated cells and 23.1% ± 2.1% for rosiglitazone plus valproic acid-treated cells) and PC3 cells (12.6% ± 2.1% for vehicle-treated cells versus 2.1% ± 0.8% for pioglitazone plus valproic acid-treated cells and 1.6% ± 0.7% for rosiglitazone plus valproic acid-treated cells), respectively. Flow cytometry analysis further demonstrated the antiproliferative effect of our treatments on PC3 cells, showing a decrease in the number of cells in the S phase concomitant to an increase in the proportion of cells in the G_1 phase of the cell cycle compared to vehicle-treated cells (Fig. 1D). Similarly to BrdU incorporation studies, the combination therapy resulted in the highest accumulation of cells in the G_1 phase of the cell cycle (Fig. 1D). These results suggest an inhibitory effect of the combined treatment of PPARγ agonists and valproic acid on cellular proliferation of several prostate cancer cell lines. Moreover, the effects of the treatment are independent of the AR status of the cells, since LNCaP and PC3 cells responded similarly to the combination therapy. Interestingly, the inhibition of proliferation following treatments was more important for LNCaP and PC3 cells than for DU145 cells. Since LNCaP and PC3 cells express wild-type Rb protein and DU145 cells express mutant Rb protein, this suggests that our treatment efficacy could depend on Rb status and might involve Rb-dependent pathways.

Next, we determined the effect of our treatments on apoptosis of PC3 prostate cancer cells. No effect was observed upon pioglitazone treatment, whereas a significant proportion of PC3 cells underwent apoptosis when treated with valproic acid or pioglitazone combined with valproic acid (Fig. 1E). Altogether, these results demonstrate that the combination treatment decreases cellular proliferation and increases apoptosis.

Regulation of expression of cell cycle regulators and pRb phosphorylation by PPARγ agonists and HDAC inhibitors in prostate cancer cells. Since pioglitazone and valproic acid treatments impact cellular proliferation of PC3 cells, we next wanted to analyze the expression of cell cycle regulators. Consistent with the observed cell cycle arrest, mRNA and protein expression of the cell cycle inhibitors p19, p21, and p27 were increased in response to pioglitazone, valproic acid, and (to a higher extent) the combination treatment (Fig. 2A and B). Moreover, cyclin D1 mRNA and protein levels were decreased upon treatment with pioglitazone alone or in combination with valproic acid (Fig. 2A and B). Previous reports demonstrated that PPARγ agonists regulate p21 expression in pancreatic and

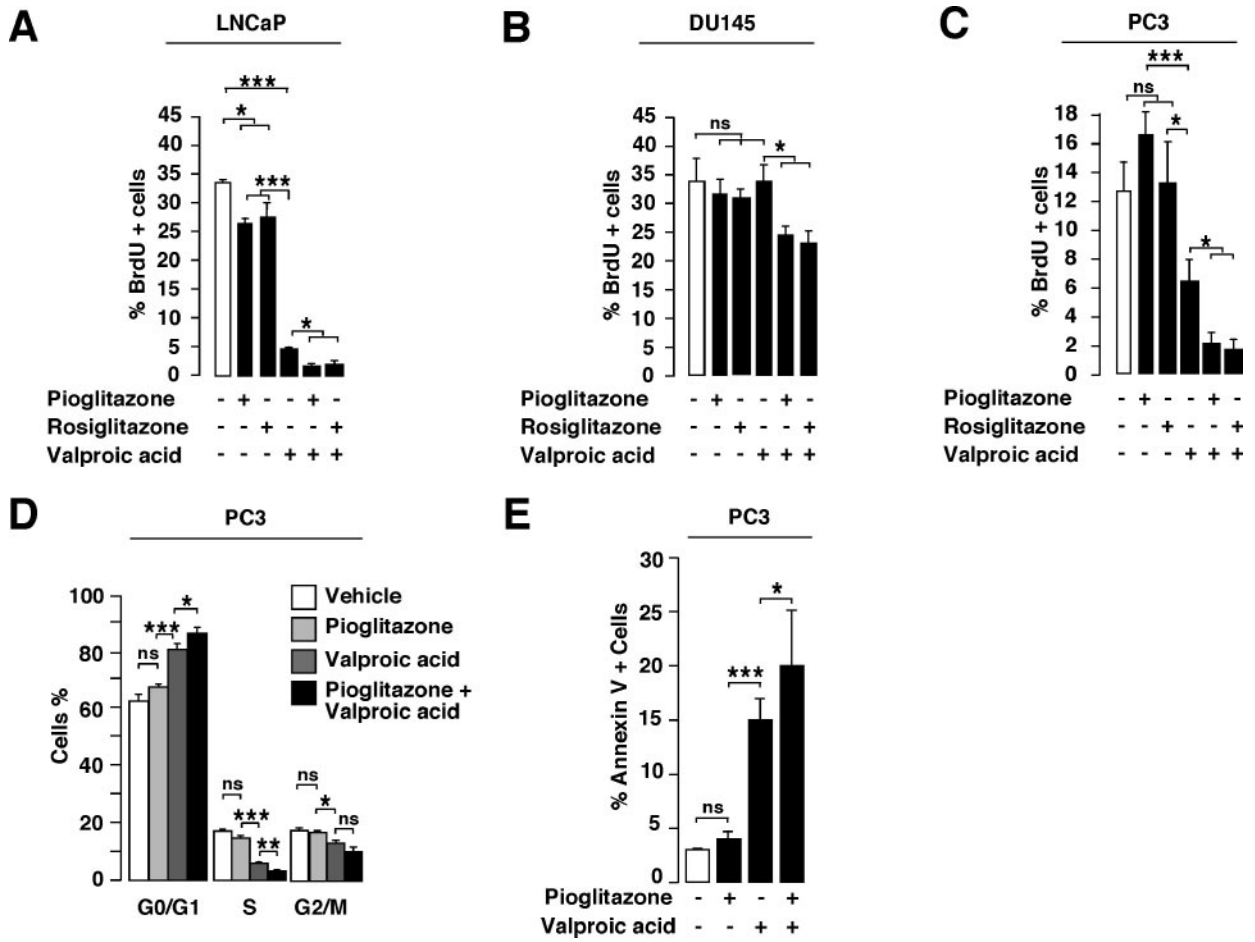

FIG. 1. Proliferation of prostate cancer cells in response to PPARγ agonists and HDAC inhibitor. (A to C) Quantification of BrdU incorporating LNCaP (A), DU145 (B), and PC3 (C) cells treated with vehicle (white bars), pioglitazone, rosiglitazone, valproic acid, or a combination of both PPARγ agonists and HDAC inhibitor. At least 500 cells were counted under a microscope. Asterisks indicate statistically significant results (analysis of variance; ns, not significant; *, $0.01 \leq P < 0.05$; **, $0.001 \leq P < 0.01$; ***, $P < 0.001$). (D) Flow cytometry analysis of PC3 cells in response to pioglitazone, valproic acid, or both. Fractions of cells in the G_0/G_1, S, or G_2/M phases of the cell cycle are indicated. (E) Quantification of apoptosis of PC3 cells in response to pioglitazone, valproic acid, or both. +, presence of agonist or inhibitor (black bars); −, absence of agonist or inhibitor (white bars).

lung cancer cells through interaction with sp1 proteins and binding to sp1 sites on the p21 promoter (13, 16). In addition, it has been demonstrated recently that rosiglitazone posttranscriptionally induces p21 in PC3 cells (28). To clarify whether the increased p21 mRNA and protein expression was mediated by PPARγ transcriptional activity or by indirect mechanisms, chromatin immunoprecipitation assays were performed. Using primers amplifying the sp1 sites in the human p21 promoter, previously shown to mediate the effects of PPARγ through sp1 binding (16), we observed that PPARγ was bound to this promoter region in PC3 cells, suggesting a transcriptional regulation of the p21 promoter by PPARγ (Fig. 2C; see Fig. S1A in the supplemental material). Moreover, we observed an increased acetylation status of histone H4 from vehicle-, pioglitazone-, valproic acid-, and pioglitazone plus valproic acid-treated cells, suggesting an increased transcriptional activity of this promoter (Fig. 2C; see Fig. S1A in the supplemental material). Since several cell cycle inhibitors are induced upon treatment, we next wanted to study the effect of our treatments on pRb phosphorylation in PC3 cells. pRb phosphorylation levels were dramatically decreased, as assessed by immunofluorescence assays (Fig. 2D). Moreover, using an anti-pRb antibody detecting unphosphorylated and phosphorylated pRb proteins and an anti-^{P}pRb antibody detecting only the Ser 807/811 phosphorylated form of pRb, we observed by immunoblotting a decrease in ^{P}pRb in cells treated with pioglitazone, valproic acid, or both and an accumulation of unphosphorylated pRb from nontreated to pioglitazone plus valproic acid-treated cells, which was consistent with arrested proliferation (Fig. 2E). To further assess the participation of the CDK4/cyclin D complex in pRb phosphorylation upon treatments, kinase activity experiments were performed. Immunoprecipitated CDK4 from PC3 cells treated with vehicle was active in nontreated cells, whereas it was inactive in cells treated with pioglitazone, valproic acid, or both (Fig. 2F). Altogether, these results demonstrate that the observed decreased cellular proliferation of PC3 cells upon treatments could be the result of an in-

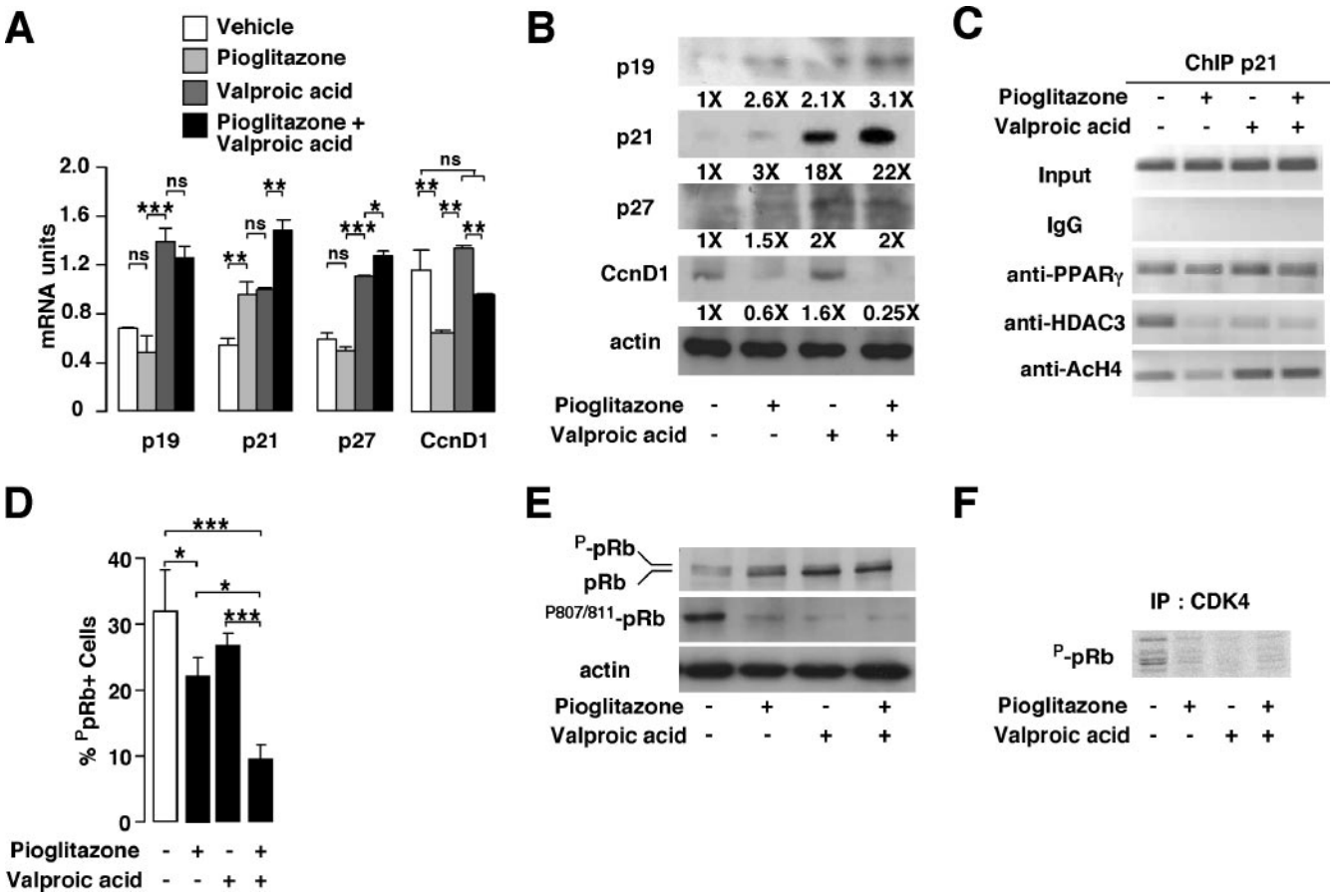

FIG. 2. Analysis of cell cycle regulators in response to PPARγ agonist and HDAC inhibitor. (A) Quantification by Q-PCR of mRNA expression of the indicated genes in PC3 cells in response to pioglitazone, valproic acid, or both. Results were normalized for expression of RS9 mRNA. CcnD1, cyclin D1. (B) Immunoblotting of the indicated proteins in PC3 cells treated as indicated in panel A. The corresponding induction (*n*-fold) compared to that for nontreated cells is indicated below the image. (C) Results from ChIP assays, showing binding of PPARγ and HDAC3 to the human p21 promoter in a region containing sp1 sites and the presence of acetylated histone H4 in this region. PC3 cells were treated as indicated in panel A. (D) Quantification of pRb phosphorylation levels in PC3 cells following treatment as indicated (white bar, no treatment). At least 500 cells were counted under a fluorescence microscope for detection of phospho-pRb after use of an anti-phospho-Rb antibody. (E) Western blot analysis of PC3 whole-cell extracts treated as indicated in panel A. The proteins detected with specific antibodies are indicated. (F) CDK4 activity in PC3 cells. Results from sodium dodecyl sulfate-polyacrylamide gel electrophoresis autoradiography show phosphorylated, purified pRb by immunoprecipitated (IP) CDK4 from vehicle-, pioglitazone-, valproic acid-, and pioglitazone plus valproic acid-treated PC3 cells. See the legend for Fig. 1 for definitions of symbols.

creased expression of cell cycle inhibitors, leading to reduced pRb phosphorylation levels.

Inhibition of tumor progression in a mouse model of prostate cancer in response to pioglitazone and valproic acid combination therapy. To evaluate the in vivo effect of a combined therapy of pioglitazone and valproic acid on prostate cancer development, we used an immunodeficient mouse model in which luminescent PC3 cells were grafted subcutaneously, allowing us to follow tumor initiation and progression by using bioluminescent imaging. We observed no failure in tumor initiation, with 100% of grafted cells giving rise to a tumor. No significant differences in tumor volume and mass were observed for mice treated with either pioglitazone or valproic acid, whereas a 40% decrease in tumor volume and mass was observed for mice treated with the combination of pioglitazone and valproic acid compared to mice treated with vehicle (Fig. 3A and B). Consistent with the inhibition of tumor growth, a decrease in cell proliferation in tumors of mice treated with the combination therapy compared to that in tumors of mice treated with vehicle was observed, as measured by PCNA staining on histological sections of the tumors (Fig. 3C and D). Consistent with the sizes of tumors (Fig. 3A and B), no effect on tumor cell proliferation was observed when each single agent (pioglitazone or valproic acid) was used in the treatment. Further characterization indicated that the expression of p21 was increased in tumors of mice treated with the combination therapy compared to expression in tumors of mice treated with vehicle or single-agent therapy (Fig. 3E and F), consistent with the observed decrease in cell proliferation. Interestingly, when analyzing other markers of tumor aggressiveness in mice treated with the combination therapy we found increased expression of E-cadherin, which is important in the control of invasion and migration of cancer cells (Fig. 3G).

Decreased in vitro and in vivo invasion potential of prostate cancer cells treated with pioglitazone and valproic acid. Increased expression of E-cadherin suggested that the combina-

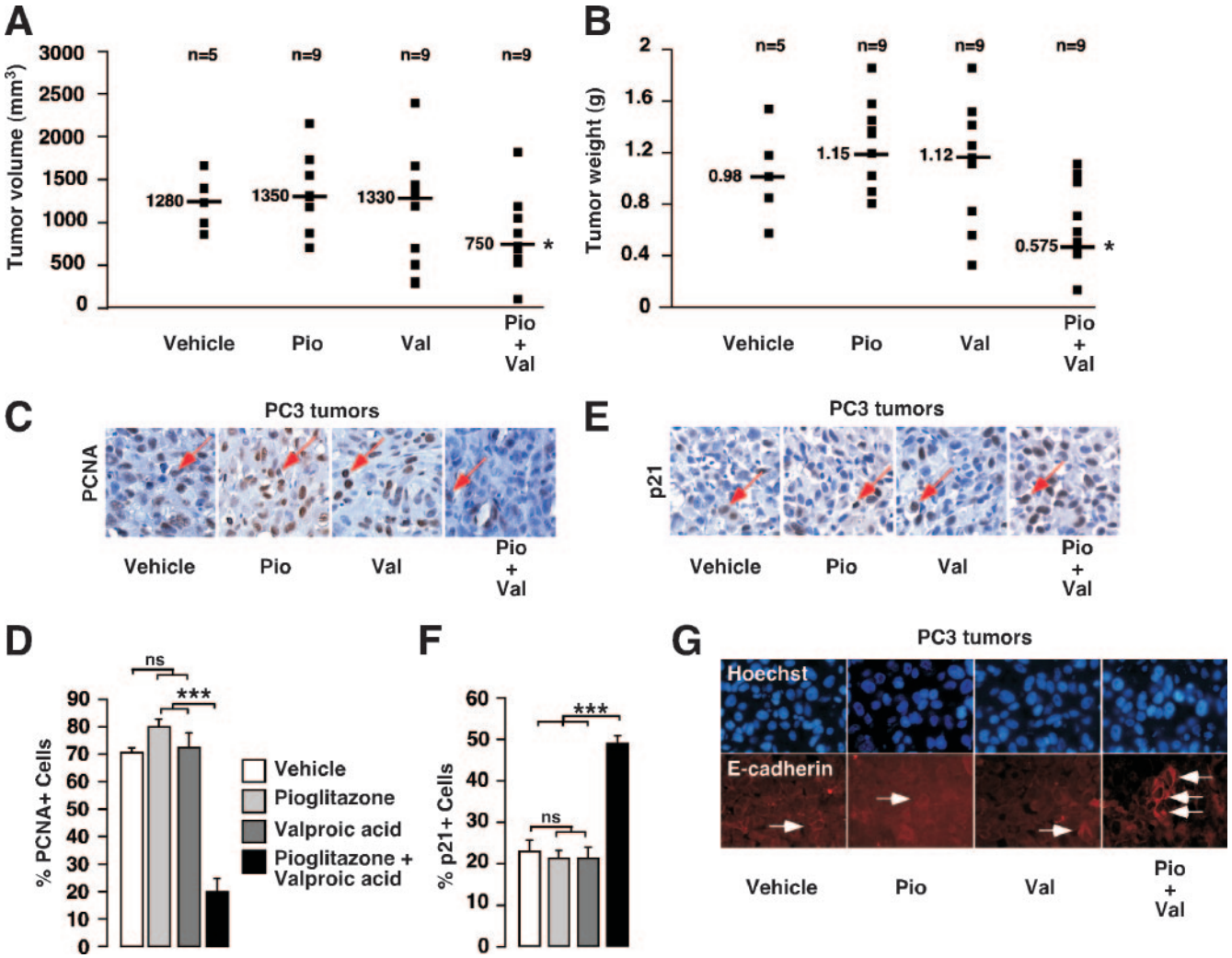

FIG. 3. In vivo analysis of tumor development in nude mice in response to pioglitazone and valproic acid after PC3 cell graft. (A and B) Volumes (A) and weights (B) of luminescent PC3 tumors in nude mice treated for 4 weeks with vehicle, pioglitazone (Pio), valproic acid (Val), or both (Pio+Val), as described in Materials and Methods. The number of mice used and the median value for each group are indicated. (C) Micrography representative of PCNA staining (red arrow) by IHC of tumor sections in mice treated with vehicle, pioglitazone, valproic acid, or both. (D) Quantification of PCNA staining represented in panel C. Four fields per section were analyzed for PCNA staining indicative of cell proliferation. Sections of tumors of all mice were analyzed. At least 500 cells were counted per tumor. (E) Micrography representative of p21 staining (red arrow) by IHC of tumor sections in mice treated with vehicle, pioglitazone, valproic acid, or both. (F) Quantification of p21 staining represented in panel E was obtained as described for panel D. (G) Micrography representative of E-cadherin staining by immunofluorescence (white arrow) of sections of tumors in mice treated with vehicle, pioglitazone, valproic acid, or both. See legend for Fig. 1 for definitions of other symbols.

tion treatment could have an impact on the invasion and migration potential of prostate cancer cells. We therefore evaluated the effect of the combination of pioglitazone and valproic acid on the invasiveness of LNCaP and PC3 cells by using a Matrigel assay. Treatments of LNCaP cells with pioglitazone, valproic acid, or both had no effect on the invasive potential of these cells (Fig. 4A), probably due to the low metastatic potential of this cell line (17, 27) and a weak percentage of cells invading the Matrigel membrane under basal conditions (Fig. 4A). In PC3 cells, which have a high metastatic potential (20, 27), pioglitazone treatment showed no significant effect on invasiveness of the cells compared to that of the control vehicle-treated cells (41.9% ± 2.0% for control-treated cells versus 32.2% ± 8.6% for pioglitazone-treated cells), whereas decreased invasion was observed when PC3 cells were treated with valproic acid (24.0% ± 2.3%). Strikingly, a synergistic effect on the inhibition of invasion was observed when a combination of pioglitazone and valproic acid was used (11.4% ± 3.1%). These results suggested that the invasion potential of highly metastatic prostate cancer cells was inhibited in the presence of the combination treatment.

These data prompted us to study the effect of pioglitazone and valproic acid on the inhibition of invasion in vivo. Prostate cancer cells preferentially invade bone. We therefore used a bone invasion model by intratibially injecting luminescent PC3 cells in immunodeficient mice. Mice were treated thereafter for 30 days with the combination therapy pioglitazone and valproic acid. In vivo imaging techniques using a charge-cou-

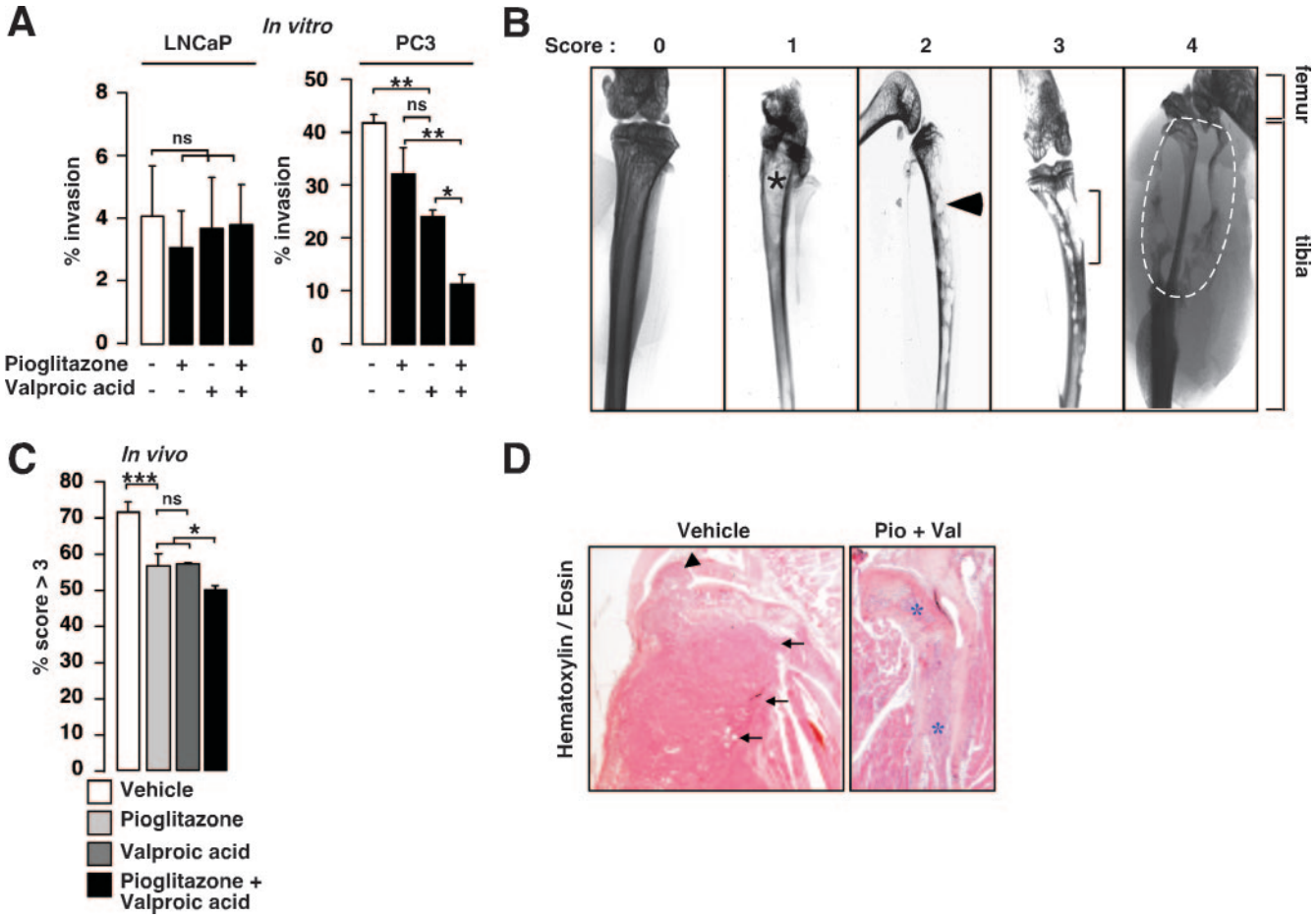

FIG. 4. Analysis of invasive potential of prostate cancer cells both in vitro and in vivo in response to valproic acid and pioglitazone treatments. (A) Invasive capacity of LNCaP and PC3 cells in Matrigel-coated membrane in response to pioglitazone, valproic acid, or both, as indicated. Percent invasion represents the proportion of plated cells that migrated through the membrane. White bars, no treatment. (B) Representative X-ray analysis and scores of the PC3-engrafted tibiae of SCID mice after 21 days of treatment with vehicle, pioglitazone, valproic acid, or a combination of pioglitazone and valproic acid. Xenografted tibiae were scored from 0 to 4 depending on the invasion degree: 0, no invasion; 1, weak and localized sign of invasion (asterisk); 2, regular features of invasion (arrowhead); 3, strong marks of bone destruction (bracket); 4, complete bone destruction (inside the white dotted line). Locations of femur and tibia bone structures are indicated. (C) Qualitative in vivo invasion analysis of X ray. X-ray radiographs were blindly scored for bone invasion potential, and results are presented as relative percentages of scores of >3. (D) Hematoxylin and eosin staining of intratibial tumors, demonstrating invasion of tumor cells from mice treated with vehicle in the join (large arrowhead) and in the skeletal muscle (small arrowheads), whereas PC3 tumors from pioglitazone plus valproic acid (Pio+Val)-treated mice remained in the bone cavity (asterisks). See legend for Fig. 1 for definitions of other symbols.

pled-device camera facilitated the follow-up of tumor initiation and growth in these animals by quantification of the luciferase signal after intraperitoneal luciferin injection. As described for subcutaneous xenograft, no failure in tumor initiation was observed. To characterize the in vivo bone invasion potential of our xenografted PC3 cells, X-ray analysis of the legs was performed and bone destruction was scored from 0 (no destruction and thus no invasion) to 4 (high degree of bone destruction, demonstrating a high invasion potential) (Fig. 4B). X-ray analysis of treated mice showed preservation of bone structure and density, whereas massive bone destruction was observed for nontreated mice (Fig. 4C). Moreover, histological analysis of the tibiae demonstrated that tumor cells engrafted in mice treated with vehicle destroyed the tibial bone and spread both in the join and in the skeletal muscle, whereas PC3 cells from pioglitazone plus valproic acid-treated mice remained inside the central bone cavity (Fig. 4D), reinforcing the scoring data presented in Fig. 4C. These results demonstrate that the combination of pioglitazone and valproic acid is effective in the inhibition of invasion of prostate cancer cells in bone.

Increased expression of E-cadherin mRNA in prostate cancer cells in response to pioglitazone and valproic acid treatment. Inhibition of invasion of prostate cancer cells was likely the result, at least in part, of increased expression of E-cadherin. Since PPARγ and HDAC are key regulators of gene transcription, we tested the hypothesis that E-cadherin expression could be regulated at the transcriptional level by pioglitazone and valproic acid. With LNCaP cells, we failed to induce E-cadherin mRNA expression upon addition of pioglitazone, valproic acid, or both, suggesting that in this cell line PPARγ might have no transcriptional effect on genes involved in migration processes (Fig. 5A, LNCaP). This idea is rein-

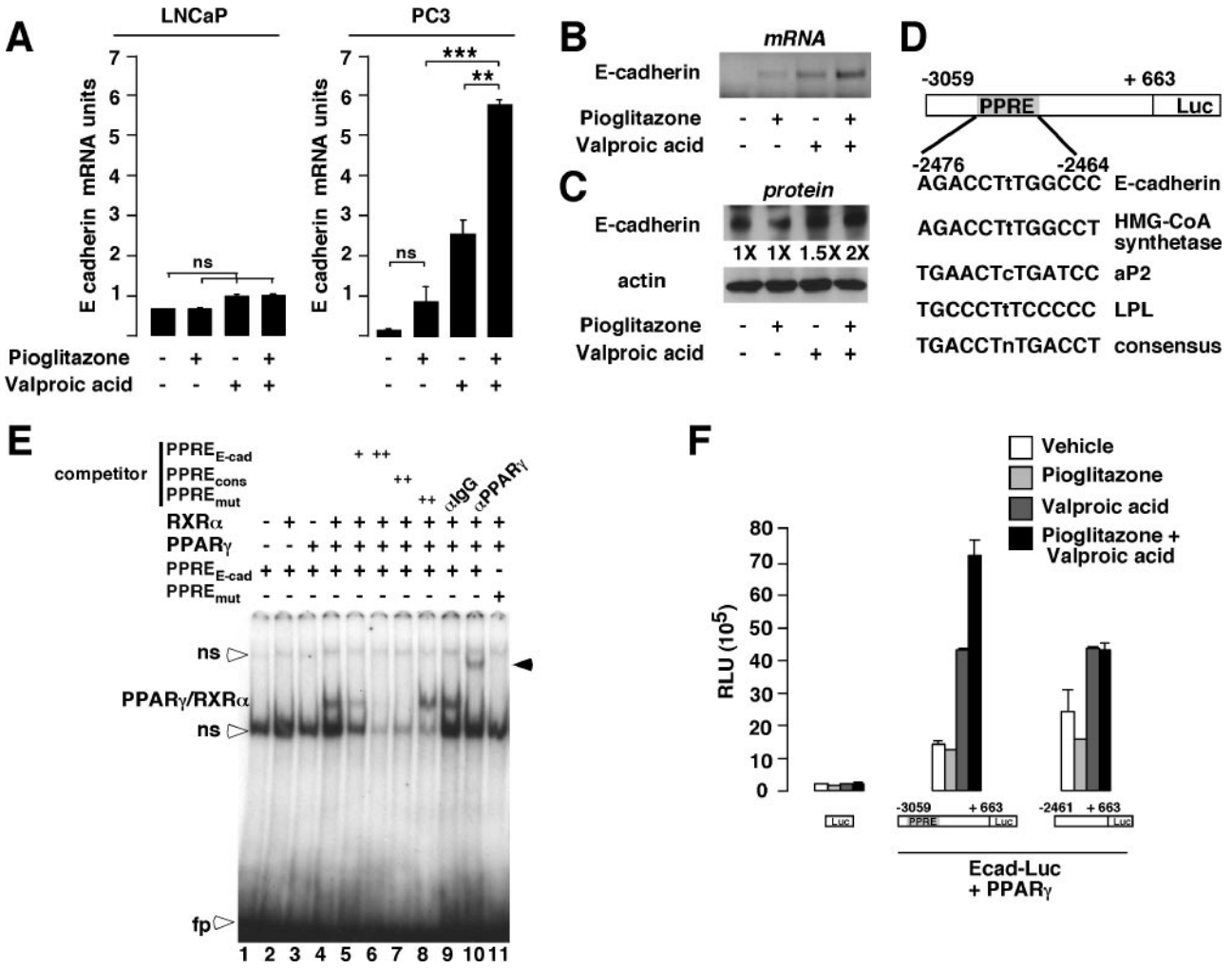

FIG. 5. E-cadherin expression, in vitro binding by PPARγ/RXRα, and transactivation assays in response to pioglitazone and/or valproic acid treatments. (A) Quantification of mRNA expression by Q-PCR of the E-cadherin gene in LNCaP and PC3 cells in response to pioglitazone, valproic acid, or both. Results were normalized for expression of RS9 mRNA. (B) Semiquantitative RT-PCR imaging showing expression of the E-cadherin mRNA in PC3 cells in response to pioglitazone, valproic acid, or both. (C) Western blot analysis of PC3 whole-cell extracts treated as indicated in panel A. The proteins detected with specific antibodies and the levels of induction (*n*-fold) are indicated. (D) Computational analysis of the regulatory region of the human E-cadherin gene demonstrating the presence of a potential PPRE. Comparison of this PPRE with the PPREs of classical PPARγ target genes is illustrated. (E) In vitro binding of the PPARγ/RXRα heterodimer to the E-cadherin promoter. EMSA analysis of the radiolabeled PPRE of the E-cadherin promoter incubated with unprogrammed reticulocyte lysate (lane 1), in vitro-translated RXRα (lane 2), PPARγ (lane 3), or both (lane 4 to 11). Double-stranded cold oligonucleotides, representing the E-cadherin PPRE ($PPRE_{E\text{-}cad}$), the consensus PPRE ($PPRE_{cons}$), or the mutated E-cadherin PPRE ($PPRE_{mut}$), were included in the competition assays (lanes 5 to 8). Incubation of an anti-PPARγ antibody resulted in a supershifted band (lane 10, black arrowhead), whereas no modification in PPARγ/RXRα binding was observed with IgG (lane 9). No binding was observed when a radiolabeled mutated E-cadherin PPRE ($PPRE_{mut}$) was used as a probe (lane 11). ns, nonspecific binding; fp, free probe. (F) Pioglitazone and valproic acid treatments modulate E-cadherin promoter activity. Shown are relative luciferase activities as determined after cotransfection of COS cells with the PPARγ expression vector and the empty construct, the E-cadherin promoter construct, or the E-cadherin promoter deletion mutant reporter construct. Cells were treated as indicated. Luc, luciferase; HMG-CoA synthetase, 3-hydroxy-3-methylglutaryl coenzyme A synthetase; LPL, lipoprotein lipase; RLU, relative luciferase units; Ecad-Luc, E-cadherin luciferase reporter. See legend for Fig. 1 for definitions of symbols.

forced by the invasion results showing that migration of LNCaP cells is not modified upon treatment with PPARγ agonists or HDAC inhibitor (Fig. 4A). In the androgen-independent and highly metastatic PC3 cell line, no significant induction of E-cadherin mRNA levels was observed after pioglitazone treatment of PC3 cells. In contrast, valproic acid significantly induced E-cadherin mRNA up to 10-fold compared to results with vehicle-treated cells (Fig. 5A and B). Interestingly, the combination of pioglitazone and valproic acid further increased E-cadherin mRNA expression (70-fold induction) (Q-PCR [Fig. 5A] and semiquantitative RT-PCR [Fig. 5B]). Consistent with the mRNA data, the association of pioglitazone and valproic acid resulted in an increase in E-cadherin protein levels compared to results with vehicle-treated PC3 cells (Fig. 5C).

Computational analysis of the E-cadherin promoter identified a PPRE, located at nucleotides −2476 to −2464 from the transcription initiation start site, that was highly conserved

compared to the PPRE found in PPARγ target genes, such as the 3-hydroxy-3-methylglutaryl coenzyme A synthetase, the aP2, and the lipoprotein lipase promoters (Fig. 5D). EMSA analysis using the PPRE found in the E-cadherin gene as a probe indicated that the in vitro-translated PPARγ/RXRα heterodimer specifically bound to this element, as demonstrated by the use of a competitor probe containing a consensus PPRE and the use of a PPARγ antibody, which supershifted the retarded PPARγ-containing band (Fig. 5E). No binding was observed when the reticulocyte lysate or the in vitro-translated PPARγ or RXRα was used alone (Fig. 5E, lanes 1, 2, and 3). These results suggested that the PPARγ/RXRa heterodimer could regulate the expression of E-cadherin through direct binding to its promoter.

To determine whether PPARγ/RXRα could activate the human E-cadherin promoter in vitro, COS cells were cotransfected with a PPARγ expression vector and with the full-length E-cadherin promoter containing the PPRE driving the expression of the luciferase gene or a deletion mutant devoid of this PPRE. No effect of pioglitazone on E-cadherin promoter activity was observed in the presence of PPARγ expression vectors, whereas valproic acid induced up to threefold E-cadherin promoter activity. Consistent with increased E-cadherin mRNA expression (Fig. 5A and B), the combination of pioglitazone and valproic acid had synergistic effects and induced up to fivefold the activity of the full-length E-cadherin promoter in COS cells (Fig. 5F). This synergistic effect was abrogated when the PPRE of the E-cadherin promoter was deleted (Fig. 5F), suggesting that PPARγ was mediating the synergistic effects. The same results were obtained when PC3 cells were transiently transfected (data not shown). Interestingly, the E-cadherin gene contains a functional PPRE that is responsive to PPARγ but only in the presence of HDAC inhibitors.

Regulation of E-cadherin expression defines a new class of PPARγ target genes responding only to the combination treatment. To further elucidate the molecular mechanisms underlying the effect of PPARγ on the expression of E-cadherin discussed above, we first tested the presence of the HDAC3 repressor protein in the PPARγ complex in PC3 cells by coimmunoprecipitation studies. We first verified that our treatments had no impact on PPARγ and HDAC3 protein levels, as demonstrated by immunoblotting (Fig. 6A). When protein extracts from PC3 cells were immunoprecipitated using an anti-HDAC3 antibody, endogenous PPARγ protein was associated with HDAC3 in the control-, pioglitazone-, and valproic acid-treated cells and was minimally detected in cells cotreated with pioglitazone and valproic acid (Fig. 6B). To further prove that HDAC3 is associated with PPARγ and represses its transcriptional activity, chromatin immunoprecipitation studies of the E-cadherin promoter were performed. A 414-bp fragment of the human E-cadherin promoter containing the binding site of PPARγ was amplified by PCR when anti-PPARγ was used to immunoprecipitate chromatin from vehicle-, pioglitazone-, valproic acid-, and pioglitazone plus valproic acid-treated cells (Fig. 6C, PPRE, and Fig. S1B in the supplemental material). Interestingly, a PCR amplification product was observed when anti-HDAC3 was used to immunoprecipitate chromatin from vehicle-, pioglitazone-, or valproic acid-treated cells, whereas no amplification was observed when immunoprecipitated chromatin from cells treated with the combination of pioglitazone and valproic acid was used as a template or when nonspecific IgGs were used to immunoprecipitate the chromatin (Fig. 6C, PPRE, and Fig. S1B in the supplemental material). Moreover, when an anti-acetylated histone H4 antibody was used, the E-cadherin promoter could be amplified in valproic acid-treated and pioglitazone plus valproic acid-treated cells, indicating that, under these conditions, the E-cadherin promoter was activated (Fig. 6C, PPRE, and Fig. S1B in the supplemental material). Binding of PPARγ and HDAC3 was specific to the PPARγ binding site of the E-cadherin promoter, since no amplification of a promoter region located outside the PPRE was observed (Fig. 6C, non PPRE). However, when chromatin was immunoprecipitated using an anti-acetylated histone H4, we observed amplification of the region devoid of the PPRE after treatments of the cells with valproic acid and pioglitazone plus valproic acid and, to a much lesser extent, after treatment with pioglitazone, suggesting that this region is also transcriptionally active (Fig. 6C, non PPRE). To further prove the direct association of HDAC3 with PPARγ on the E-cadherin promoter, we performed Re-ChIP experiments. After a first chromatin immunoprecipitation using an anti-PPARγ antibody, we performed a second immunoprecipitation using an anti-HDAC3 antibody or nonspecific IgGs. As observed for ChIP experiments, the same fragment of the human E-cadherin promoter was amplified by PCR when anti-HDAC3 was used to immunoprecipitate chromatin from vehicle-, pioglitazone-, or valproic acid-treated cells (Fig. 6D and Fig. S1C in the supplemental material), demonstrating that HDAC3 forms a complex with PPARγ in PC3 cells on the E-cadherin promoter even in the presence of valproic acid. No association of PPARγ and HDAC3 with the E-cadherin promoter was observed when chromatin from cells treated with a combination of pioglitazone and valproic acid was used (Fig. 6D and Fig. S1C in the supplemental material).

Finally, we asked whether other known PPARγ target genes, such as aP2, responded to the treatments similarly to E-cadherin. In contrast to what we observed for the E-cadherin gene, aP2 mRNA expression was induced more than 100-fold in PC3 cells treated with pioglitazone compared to cells treated with vehicle (Fig. 6E). Surprisingly, only minor effects on aP2 mRNA expression were observed upon treatment with valproic acid (Fig. 6E). Furthermore, combination treatment of pioglitazone and valproic acid induced aP2 mRNA expression at levels similar to those observed for pioglitazone treatment alone (Fig. 6E). These results suggested that PPARγ differentially regulated transcription in the contexts of the E-cadherin and the aP2 genes. Transient-transfection assays with COS and PC3 (data not shown) cells using the aP2 luciferase-based promoter construct were consistent with this hypothesis. As observed for the aP2 mRNA expression, pioglitazone induced the aP2 promoter activity, whereas no effect on luciferase activity was observed upon valproic acid treatment (Fig. 6F). Moreover, no additive effect of the association of pioglitazone and valproic acid on luciferase activity was observed for this promoter (Fig. 6F). To elucidate the molecular mechanism underlying the observed effects, Re-ChIP experiments were performed with the aP2 gene as described above. A 567-bp fragment of the human aP2 promoter containing the PPRE was amplified by PCR when anti-HDAC3 was used to reimmunoprecipitate PPARγ-immunoprecipitated chromatin from

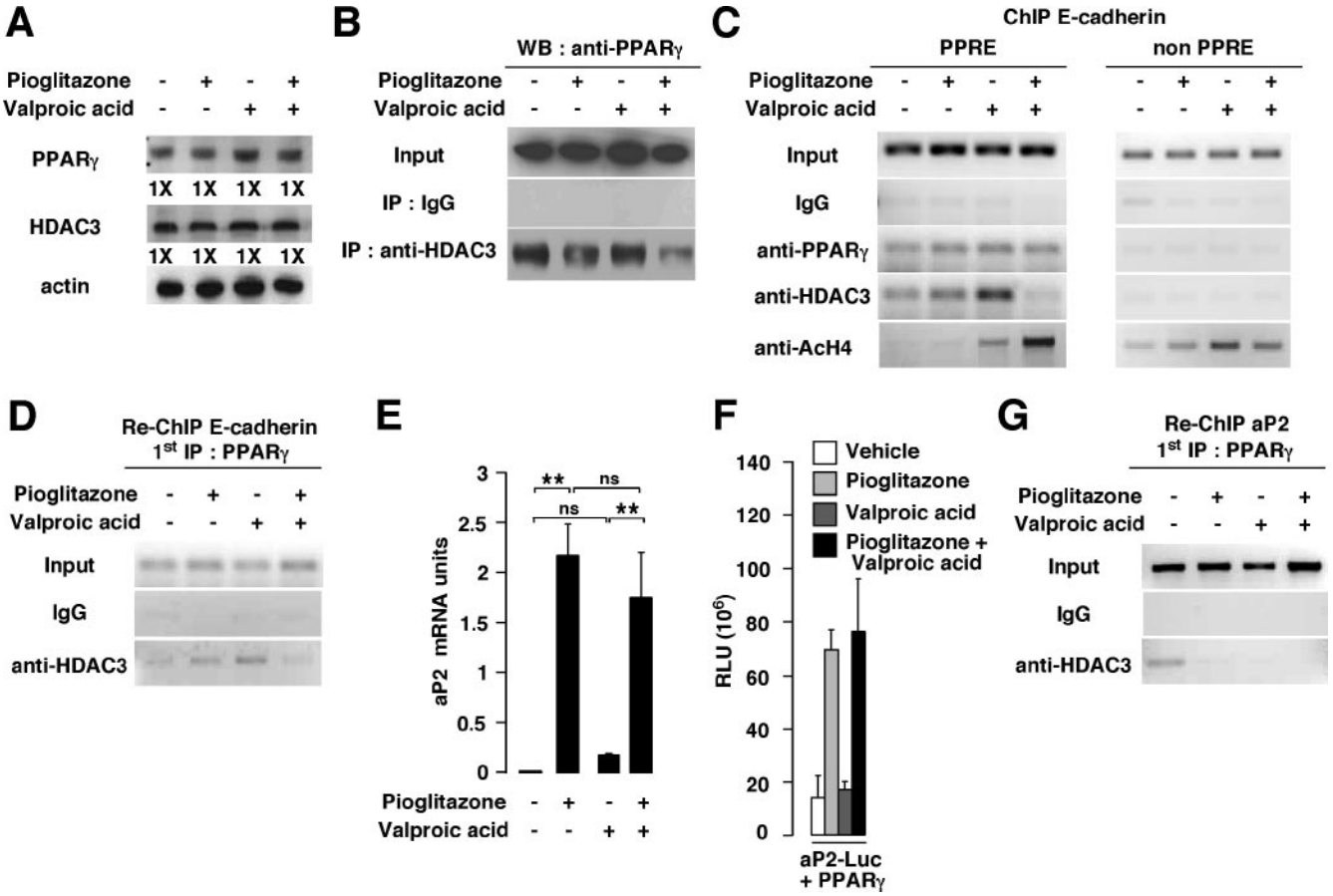

FIG. 6. Differential HDAC3 recruitment and in vivo binding of PPARγ to the E-cadherin and aP2 promoters in response to pioglitazone and/or valproic acid treatments. (A) Western blot showing PPARγ and HDAC3 expression in PC3 cells treated with pioglitazone, valproic acid, or both. Induction (*n*-fold) is indicated. (B) Immunoprecipitation (IP) assays showing interaction between PPARγ and HDAC3. Extracts from PC3 cells treated with vehicle, pioglitazone, valproic acid, or both were immunoprecipitated with IgG or anti-HDAC3 or directly analyzed for the presence of PPARγ (Input). Western blot analysis revealed the presence of PPARγ in HDAC3 immunoprecipitates. (C) ChIP demonstrating binding of PPARγ and HDAC3 to the E-cadherin promoter. Cross-linked chromatin from PC3 cells treated with vehicle, pioglitazone, valproic acid, or both was incubated with antibodies against PPARγ, HDAC3, acetylated H4, or IgG. Immunoprecipitates were analyzed by PCR using specific primers for the PPRE present in the E-cadherin promoter (PPRE) or primers amplifying a region outside the PPRE (non PPRE). As a control, a sample representing 10% of the total chromatin was included in the PCR (Input). (D) Re-ChIP assays demonstrating interaction between HDAC3 and PPARγ on the E-cadherin promoter. Chromatin prepared from PC3 cells treated with vehicle, pioglitazone, valproic acid, or both was subjected to the ChIP procedure with the antibody against PPARγ and reimmunoprecipitated using IgG or anti-HDAC3 antibody. Immunoprecipitates were analyzed as described for panel C. (E) Quantification of mRNA expression by Q-PCR of the aP2 gene in PC3 cells in response to pioglitazone, valproic acid, or both. Results were normalized for expression of RS9 mRNA. (F) Activity generated by the aP2 luciferase (aP2-Luc) reporter cotransfected with the PPARγ expression vector. Experiments were performed either without stimulation (vehicle) or in the presence of pioglitazone, valproic acid, or both. (G) Re-ChIP assays demonstrating interaction between HDAC3 and PPARγ on the aP2 promoter. Chromatin was prepared and subjected to the Re-ChIP procedure as described for panel D. Immunoprecipitates were analyzed using primers specific for the aP2 promoter. WB, Western blot; RLU, relative luciferase units. See the legend for Fig. 1 for definitions of symbols.

vehicle-treated PC3 cells (Fig. 6G and Fig. S1D in the supplemental material). In contrast to the E-cadherin gene promoter, HDAC3 was not present on the aP2 promoter of PC3 cells treated with pioglitazone, valproic acid, or both, suggesting that HDAC3 is not associated with PPARγ under these conditions on the aP2 promoter (Fig. 6G and Fig. S1D in the supplemental material). Altogether, our data suggest that the E-cadherin and aP2 genes are differentially transcriptionally regulated by PPARγ. Regulation of E-cadherin expression by PPARγ requires inhibition of HDAC regardless of the presence of PPARγ ligands, whereas in the context of the aP2 promoter, PPARγ ligands are sufficient to induce expression.

HDAC3 mediates repressive effects on PPARγ-mediated E-cadherin promoter activity. We observed by ChIP experiments that HDAC3 is recruited on the E-cadherin promoter upon pioglitazone or valproic acid treatment. To further prove that HDAC3 mediates repressive effects on the E-cadherin promoter, we first evaluated the effect of the transient overexpression of HDAC3 on PPARγ-mediated E-cadherin promoter activity. COS cells were transiently cotransfected with the PPARγ expression vector, the full-length E-cadherin promoter driving the expression of the luciferase gene, and increasing amounts of the HDAC3 expression vector (Fig. 7A). The combination of pioglitazone and valproic acid induced the E-cad-

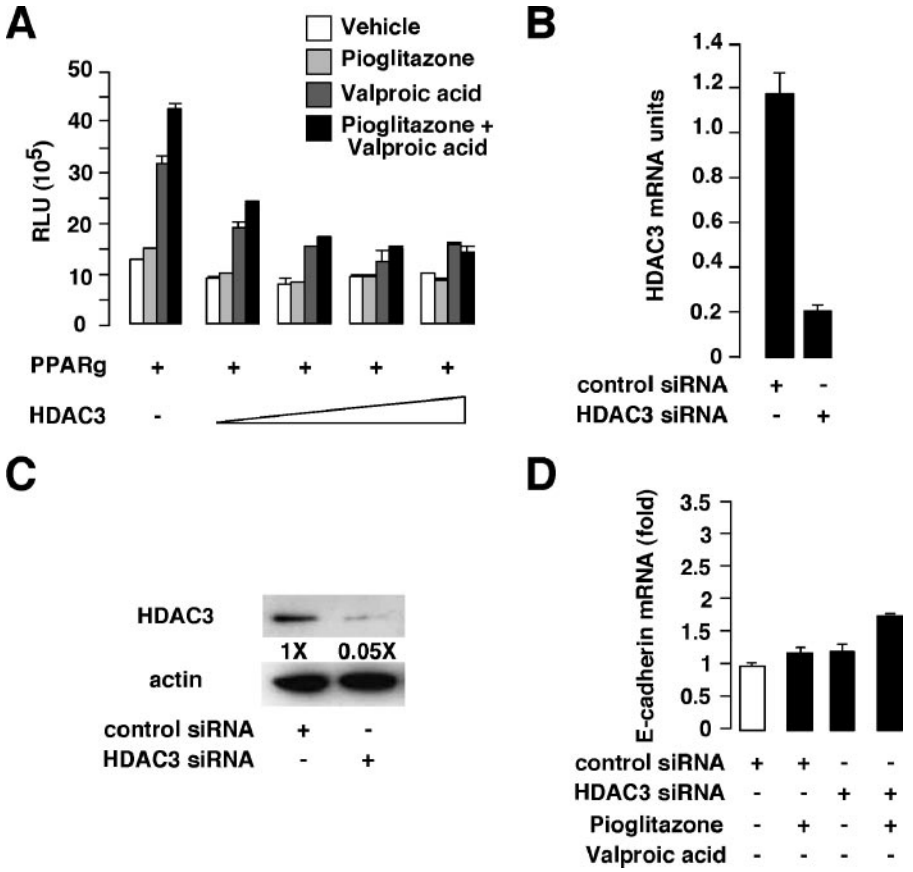

FIG. 7. Effects of HDAC3 overexpression on the E-cadherin promoter and HDAC3 knockdown on E-cadherin mRNA in response to pioglitazone. (A) Activity generated by the E-cadherin luciferase reporter cotransfected with the PPARγ expression vector and increasing amounts of the HDAC3 expression vector. Experiments were performed without stimulation (vehicle) or in the presence of pioglitazone, valproic acid, or both. (B and C) Q-PCR (B) and Western blot (C) analysis showing knockdown expression of HDAC3 expression in PC3 cells transfected with a control or HDAC3 siRNA. In panel C, levels of induction (*n*-fold) are indicated. (D) Quantitative real-time PCR showing E-cadherin gene expression in control versus HDAC3 knockdown in PC3 cells treated as indicated. RLU, relative luciferase units; +, presence of agonist or inhibitor; −, absence of agonist or inhibitor (white bar).

herin promoter activity in the absence of HDAC3 (Fig. 5E and 7A). Interestingly, when increasing amounts of HDAC3 were cotransfected with PPARγ, a strong decrease in the E-cadherin promoter activity was obtained, suggesting a repressive role for HDAC3 on the E-cadherin gene (Fig. 7A). To specifically evaluate the consequence of loss of HDAC3 expression, siRNA experiments were performed. Transfection of validated HDAC3 siRNA in PC3 cells resulted in an 80% reduction in endogenous HDAC3 mRNA and protein levels, as demonstrated by Q-PCR and immunoblotting (Fig. 7B and C, respectively). siRNA-mediated HDAC3 knockdown increased endogenous E-cadherin mRNA expression in PC3 cells treated with pioglitazone (twofold induction) (Fig. 7D), whereas no effect of pioglitazone was observed with the control siRNA (Fig. 7D). These results suggest that HDAC3 represses PPARγ transcriptional activity on the E-cadherin gene in PC3 cells upon pioglitazone treatment.

E-cadherin expression is decreased whereas PPARγ expression and deacetylated histone H4 are increased in human prostate cancer. One important requirement in order to ensure a successful therapy using a combination of PPARγ agonists and HDAC inhibitors is that PPARγ is expressed in prostate cancer and that histones are deacetylated. Consistent with previous studies (32), we found by IHC studies that PPARγ was mainly not expressed in normal prostate (Fig. 8A). PPARγ expression was absent in 42.9% and 65.5% of normal prostate and benign prostate hyperplasia tissues, respectively, and 42.9% of normal prostate tissues expressed low levels of PPARγ (Fig. 8A and Table 1). However, strong expression was found in prostate cancer, with 100% of prostate cancers expressing PPARγ at different levels (Fig. 8A and Table 1). Furthermore, a gradual increase in PPARγ staining was observed from differentiated (Gleason score of <7, 62.5% of cancers expressed PPARγ) to undifferentiated (Gleason score of ≥ 7, more than 80% of cancers are positive for PPARγ protein) adenocarcinomas (Table 1). In contrast to PPARγ expression, acetylation status of histone H4 was found to be inversely correlated with the aggressiveness of prostate cancer. In the normal prostate, histone H4 was often acetylated (Fig. 8B and Table 2). Eighty-one percent of normal prostate biopsy samples were positively stained (Table 2, scores 1 and 2), whereas acetylated histone H4 was mostly not detected in aggressive prostate cancer (Table 2, scores 0 and 1) (87.5%, 60%, and 78.6% of prostate cancer tissues with Gleason scores

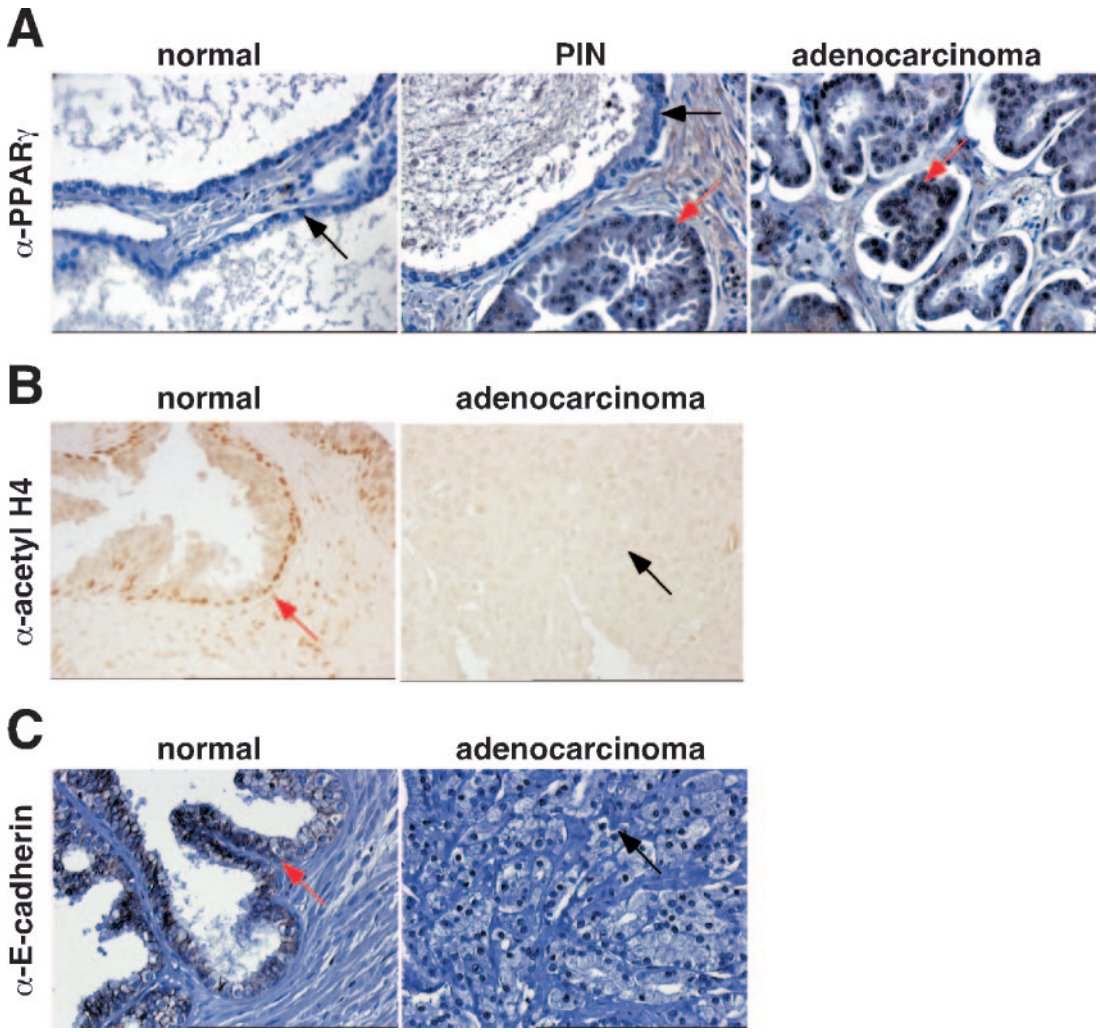

FIG. 8. Analysis of PPARγ, histone H4 acetylation, and E-cadherin expression in human normal and neoplastic prostates. (A) Micrography representative of human PPARγ staining (red arrows) by IHC of sections of normal prostate, prostatic intraepithelial neoplasia (PIN), and prostatic adenocarcinoma. Weak to no staining (black arrows) was observed in normal prostatic gland. (B) Micrography representative of acetylated histone H4 staining (red arrow) by IHC of sections of normal prostatic gland and prostatic adenocarcinoma. No immunostaining (black arrow) was observed in prostatic adenocarcinoma. (C) Micrography representative of human E-cadherin staining by IHC of tissue microarray sections of normal prostate and prostatic adenocarcinoma obtained after radical prostatectomy. Strong staining was observed in normal prostate (red arrow), whereas no staining (black arrow) was observed in adenocarcinoma.

of <7, 7, and >7 have negative or weak acetylated H4, respectively), indicating high histone deacetylase activity in prostate cancer. Furthermore, we correlated the expression of PPARγ with acetylated histone H4 in each individual tumor with different Gleason scores (Table 3). Interestingly, we found that tissues that were positively stained for both PPARγ and acetylated H4 were tumor prostates with Gleason scores of ≤7 (Table 3). In these tissues, we also observed positive staining for PPARγ and negative staining for acetylated H4 (25% of cancers with Gleason scores of <7 and 50% with Gleason

TABLE 1. PPARγ expression in normal, benign prostate hypertrophy (BPH), and prostate cancer tissues

Tissue type (total no. of samples)	No. (%) of samples with score			
	0	1	2	3
Normal (21)	9 (42.9)	9 (42.9)	3 (14.2)	0 (0)
BPH (8)	5 (65.5)	2 (25)	1 (12.5)	0 (0)
Gleason score of <7 (8)	0 (0)	3 (37.5)	5 (62.5)	0 (0)
Gleason score of 7 (10)	0 (0)	1 (10)	1 (10)	8 (80)
Gleason score of >7 (14)	0 (0)	2 (14.3)	4 (28.6)	8 (57.1)

TABLE 2. Acetylation status of histone H4 in normal, benign prostate hypertrophy (BPH), and prostate cancer tissues

Tissue type (total no. of samples)	No. (%) of samples with score			
	0	1	2	3
Normal (21)	4 (19)	7 (33.3)	10 (47.7)	0 (0)
BPH (8)	3 (37.5)	2 (25)	3 (37.5)	0 (0)
Gleason score of <7 (8)	1 (12.5)	6 (75)	1 (12.5)	0 (0)
Gleason score of 7 (10)	3 (30)	3 (30)	4 (40)	0 (0)
Gleason score of >7 (14)	6 (42.9)	5 (35.7)	3 (21.4)	0 (0)

TABLE 3. Correlation between PPARγ expression and acetylated H4 in normal, benign prostate hypertrophy (BPH), and prostate cancer tissues

Tissue type (total no. of samples)	No. (%) of samples with phenotype			
	PPARγ$^-$ AcH4$^-$	PPARγ$^-$ AcH4$^+$	PPARγ$^+$ AcH4$^-$	PPARγ$^+$ AcH4$^+$
Normal (21)	7 (33.3)	10 (47.6)	1 (4.8)	3 (14.3)
BPH (8)	3 (37.5)	2 (25)	1 (12.5)	2 (25)
Gleason score of <7 (8)	2 (25)	0 (0)	2 (25)	4 (50)
Gleason score of 7 (10)	0 (0)	0 (0)	5 (50)	5 (50)
Gleason score of >7 (14)	0 (0)	1 (7.1)	9 (64.3)	4 (28.6)

scores of 7 were PPARγ$^+$ and AcH4$^-$, respectively) (Table 3). Aggressive prostate cancers were mostly positive for PPARγ and negative for acetylated H4 (64.3% of cancers with Gleason scores of >7 were PPARγ$^+$ and AcH4$^-$) (Table 3). Most of the normal prostate tissues were negatively and positively stained for PPARγ and acetylated H4, respectively (47.6% of normal prostate were PPARγ$^-$ and AcH4$^+$) (Table 3). These data demonstrate that PPARγ expression and acetylation status of histone H4 are often inversely correlated in aggressive prostate cancer. Importantly, these results support the use of HDAC inhibitors and PPARγ agonists in the treatment of prostate cancer. Finally, consistent with previous results (19, 29), we showed that E-cadherin expression is lost in most of prostate adenocarcinoma samples (Fig. 8C), suggesting that the association of PPARγ agonists and HDAC inhibitors might be of interest to reinduce E-cadherin expression and subsequently inhibit invasion.

DISCUSSION

PPARγ is overexpressed in prostate cancer (15). Whereas the physiological function of PPARγ in normal epithelial cells is largely unknown, PPARγ activation inhibits the proliferation of malignant cells from prostate carcinoma (4, 21, 25, 34), among others. These observations suggest that induction of differentiation by activation of PPARγ may represent a promising novel therapeutic approach for cancer, as already demonstrated for liposarcoma (6) and in xenograft models of prostate (21). In addition, treatment of patients with advanced prostate cancer with the PPARγ agonist troglitazone resulted in a high incidence of stabilization of prostate-specific antigen levels (25). These studies were, however, limited to a reduced number of patients. A larger prospective, randomized, placebo-controlled clinical trial analyzed the effects of rosiglitazone on the PSA doubling time in patients with biochemical disease progression after radical prostatectomy and/or radiation therapy. In this study, no effects of rosiglitazone on disease progression were observed for these patients (35). Despite technical caveats in the interpretation of PSA doubling time measurements, this study showed that PPARγ ligands are not efficient in this subset of patients. One interesting hypothesis is that PPARγ could be insensitive to ligand activation in prostate cancer because its activity is repressed by the action of upstream events. This was demonstrated in a study showing that sustained activation of PPARγ by the new PPARγ activator R-etodolac required the presence of HER2 inhibitors, suggesting that the HER2 pathway, likely through mitogen-activated protein kinase phosphorylation of PPARγ, abrogated the effects of PPARγ activity through degradation of this nuclear receptor (14). In this scenario, PPARγ ligands cannot activate PPARγ as a result of its degradation. We show in our study that, similarly to what is observed for the HER2-PPARγ axis, inhibition of HDAC activity is required to achieve maximal PPARγ activation in prostate cancer cells. We have shown previously that PPARγ is part of an HDAC3-containing repressor complex in the presence of PPARγ ligands and we characterized a PPARγ-HDAC3 direct interaction (8). We believe that in prostate cancer cells HDAC are fully active (Fig. 8) and therefore PPARγ activity is repressed in these cells even in the presence of ligands. HDAC inhibition has been shown to result in decreased proliferation of several cancer cells (22). We found that histone H4 acetylation levels were decreased in prostate cancer tumors, although the precise correlation between histone acetylation level and tumor stage is more complex (33).

We found that PPARγ might control tumor growth at two different levels. First, this nuclear receptor might exert antiproliferative effects through regulation of the expression of cell cycle regulators. This is consistent with previous studies showing decreased expression of cyclin D1 upon PPARγ agonist treatment in cancer cell lines (38). Second, we found that the combination treatment abrogated the invasive potential of prostate cancer cells. It is known that E-cadherin is one of the major factors that inhibit metastasis and invasion of prostate cancer cells through maintenance of the adherens junctions important for epithelial cell-cell adhesion and inhibition of epithelial-to-mesenchymal transition, which is a required event in cancer progression. Downregulation of E-cadherin expression contributes to certain aspects of oncogenesis (5), and it has been observed to occur in 50% of prostate cancers (24, 36, 37). We consistently found increased expression of E-cadherin in PC3 cells treated with the combination therapy. Furthermore, we show that E-cadherin is a bona fide PPARγ target gene. In contrast to classical PPARγ target genes, regulation of E-cadherin expression in response to PPARγ ligands both at the promoter and at the RNA level requires, however, the presence of HDAC inhibitors to fully achieve maximal stimulation. This is consistent with our hypothesis that PPARγ is not permissive for activation by ligands when complexed with HDAC. This is demonstrated by our ChIP experiments, which show that despite PPARγ being bound to the promoter of the E-cadherin gene in the presence of ligand, the promoter is not active, as shown by transient-expression experiments and E-cadherin mRNA quantification. The lack of activity is most likely the result of the presence of HDAC3 in this PPARγ complex on the PPAR binding site of the E-cadherin promoter, a phenomenon that we cannot explain and are currently investigating. However, in the presence of HDAC inhibitors and PPARγ ligands, HDAC3 is absent from the PPARγ complex in the E-cadherin gene promoter, and consequently the promoter is active, as suggested by the activity of the E-cadherin promoter. The finding that E-cadherin expression responds to PPARγ agonists only in the presence of HDAC inhibitors defines a new class of PPARγ target genes.

In support of this, we show that classical PPARγ target genes, such as aP2, responded to PPARγ with a sixfold activation in the absence of HDAC inhibitors (Fig. 6). This sug-

gests that the sensitivities of PPARγ repression to HDAC are different depending on the context of the promoter of the PPARγ target gene. We can conclude from our results that a combination therapy using PPARγ agonists and HDAC inhibitors might be considered for the treatment of prostate cancer.

ACKNOWLEDGMENTS

Jacques Teyssier, Imâde Ait-Arsa, Michel Brissac, and Michelle Turmo are acknowledged for their excellent technical assistance. Members of the Equipe AVENIR and INSERM U540 are acknowledged for support and discussions.

This work was supported by grants from INSERM (Avenir), CHU de Montpellier, Association pour la Recherche contre le Cancer, Alfediam, Ligue contre le Cancer, and Fondation pour la Recherche Médicale. I.I. was supported by a grant from Ligue Nationale contre le Cancer, D.S. by the Boehringer Ingelheim Fonds Ph.D. scholarship program, and A.A. by a grant of INSERM poste vert.

REFERENCES

1. **Abella, A., P. Dubus, M. Malumbres, S. G. Rane, H. Kiyokawa, A. Sicard, F. Vignon, D. Langin, M. Barbacid, and L. Fajas.** 2005. Cdk4 promotes adipogenesis through PPARgamma activation. Cell Metab. **2:**239–249.
2. **Annicotte, J. S., C. Chavey, N. Servant, J. Teyssier, A. Bardin, A. Licznar, E. Badia, P. Pujol, F. Vignon, T. Maudelonde, G. Lazennec, V. Cavailles, and L. Fajas.** 2005. The nuclear receptor liver receptor homolog-1 is an estrogen receptor target gene. Oncogene **24:**8167–8175.
3. **Annicotte, J. S., E. Fayard, G. H. Swift, L. Selander, H. Edlund, T. Tanaka, T. Kodama, K. Schoonjans, and J. Auwerx.** 2003. Pancreatic-duodenal homeobox 1 regulates expression of liver receptor homolog 1 during pancreas development. Mol. Cell. Biol. **23:**6713–6724.
4. **Butler, R., S. H. Mitchell, D. J. Tindall, and C. Y. Young.** 2000. Nonapoptotic cell death associated with S-phase arrest of prostate cancer cells via the peroxisome proliferator-activated receptor gamma ligand, 15-deoxy-delta12,14-prostaglandin J2. Cell Growth Differ. **11:**49–61.
5. **Cano, A., M. A. Perez-Moreno, I. Rodrigo, A. Locascio, M. J. Blanco, M. G. del Barrio, F. Portillo, and M. A. Nieto.** 2000. The transcription factor snail controls epithelial-mesenchymal transitions by repressing E-cadherin expression. Nat. Cell Biol. **2:**76–83.
6. **Demetri, G. D., C. D. Fletcher, E. Mueller, P. Sarraf, R. Naujoks, N. Campbell, B. M. Spiegelman, and S. Singer.** 1999. Induction of solid tumor differentiation by the peroxisome proliferator-activated receptor-gamma ligand troglitazone in patients with liposarcoma. Proc. Natl. Acad. Sci. USA **96:**3951–3956.
7. **Fajas, L., M. B. Debril, and J. Auwerx.** 2001. Peroxisome proliferator-activated receptor-gamma: from adipogenesis to carcinogenesis. J. Mol. Endocrinol. **27:**1–9.
8. **Fajas, L., V. Egler, R. Reiter, J. Hansen, K. Kristiansen, S. Miard, and J. Auwerx.** 2002. The retinoblastoma-histone deacetylase 3 complex inhibits the peroxisome proliferator-activated receptor gamma and adipocyte differentiation. Dev. Cell **3:**903–910.
9. **Fajas, L., J. C. Fruchart, and J. Auwerx.** 1998. Transcriptional control of adipogenesis. Curr. Opin. Cell Biol. **10:**165–173.
10. **Fajas, L., R. L. Landsberg, Y. Huss-Garcia, C. Sardet, J. A. Lees, and J. Auwerx.** 2002. E2Fs regulate adipogenesis. Dev. Cell **3:**39–49.
11. **Feldman, B. J., and D. Feldman.** 2001. The development of androgen-independent prostate cancer. Nat. Rev. Cancer **1:**34–45.
12. **Glondu, M., E. Liaudet-Coopman, D. Derocq, N. Platet, H. Rochefort, and M. Garcia.** 2002. Down-regulation of cathepsin-D expression by antisense gene transfer inhibits tumor growth and experimental lung metastasis of human breast cancer cells. Oncogene **21:**5127–5134.
13. **Han, S., N. Sidell, P. B. Fisher, and J. Roman.** 2004. Up-regulation of p21 gene expression by peroxisome proliferator-activated receptor gamma in human lung carcinoma cells. Clin. Cancer Res. **10:**1911–1919.
14. **Hedvat, M., A. Jain, D. A. Carson, L. M. Leoni, G. Huang, S. Holden, D. Lu, M. Corr, W. Fox, and D. B. Agus.** 2004. Inhibition of HER-kinase activation prevents ERK-mediated degradation of PPARgamma. Cancer Cell **5:**565–574.
15. **Hisatake, J. I., T. Ikezoe, M. Carey, S. Holden, S. Tomoyasu, and H. P. Koeffler.** 2000. Down-regulation of prostate-specific antigen expression by ligands for peroxisome proliferator-activated receptor gamma in human prostate cancer. Cancer Res. **60:**5494–5498.
16. **Hong, J., I. Samudio, S. Liu, M. Abdelrahim, and S. Safe.** 2004. Peroxisome proliferator-activated receptor gamma-dependent activation of p21 in Panc-28 pancreatic cancer cells involves Sp1 and Sp4 proteins. Endocrinology **145:**5774–5785.
17. **Hoosein, N. M., D. D. Boyd, W. J. Hollas, A. Mazar, J. Henkin, and L. W. Chung.** 1991. Involvement of urokinase and its receptor in the invasiveness of human prostatic carcinoma cell lines. Cancer Commun. **3:**255–264.
18. **Huggins, C.** 1967. Endocrine-induced regression of cancers. Science **156:**1050–1054.
19. **Jaggi, M., S. L. Johansson, J. J. Baker, L. M. Smith, A. Galich, and K. C. Balaji.** 2005. Aberrant expression of E-cadherin and beta-catenin in human prostate cancer. Urol. Oncol. **23:**402–406.
20. **Keer, H. N., F. D. Gaylis, J. M. Kozlowski, H. C. Kwaan, K. D. Bauer, A. A. Sinha, and M. J. Wilson.** 1991. Heterogeneity in plasminogen activator (PA) levels in human prostate cancer cell lines: increased PA activity correlates with biologically aggressive behavior. Prostate **18:**201–214.
21. **Kubota, T., K. Koshizuka, I. A. Williamson, H. Asou, J. W. Said, S. Holden, I. Miyoshi, and H. P. Koeffler.** 1998. Ligand for peroxisome proliferator activated receptor γ (troglitazone) has potent anti-tumor effects against human prostate cancer both in vitro and in vivo. Cancer Res. **58:**3344–3352.
22. **Marks, P., R. A. Rifkind, V. M. Richon, R. Breslow, T. Miller, and W. K. Kelly.** 2001. Histone deacetylases and cancer: causes and therapies. Nat. Rev. Cancer **1:**194–202.
23. **Metivier, R., G. Penot, M. R. Hubner, G. Reid, H. Brand, M. Kos, and F. Gannon.** 2003. Estrogen receptor-alpha directs ordered, cyclical, and combinatorial recruitment of cofactors on a natural target promoter. Cell **115:**751–763.
24. **Morton, R. A., C. M. Ewing, A. Nagafuchi, S. Tsukita, and W. B. Isaacs.** 1993. Reduction of E-cadherin levels and deletion of the alpha-catenin gene in human prostate cancer cells. Cancer Res. **53:**3585–3590.
25. **Mueller, E., M. Smith, P. Sarraf, T. Kroll, A. Aiyer, D. S. Kaufman, W. Oh, G. Demetri, W. D. Figg, X. P. Zhou, C. Eng, B. M. Spiegelman, and P. W. Kantoff.** 2000. Effects of ligand activation of peroxisome proliferator-activated receptor gamma in human prostate cancer. Proc. Natl. Acad. Sci. USA **97:**10990–10995.
26. **Nelson, P. S., N. Clegg, H. Arnold, C. Ferguson, M. Bonham, J. White, L. Hood, and B. Lin.** 2002. The program of androgen-responsive genes in neoplastic prostate epithelium. Proc. Natl. Acad. Sci. USA **99:**11890–11895.
27. **Pulukuri, S. M., C. S. Gondi, S. S. Lakka, A. Jutla, N. Estes, M. Gujrati, and J. S. Rao.** 2005. RNA interference-directed knockdown of urokinase plasminogen activator and urokinase plasminogen activator receptor inhibits prostate cancer cell invasion, survival, and tumorigenicity in vivo. J. Biol. Chem. **280:**36529–36540.
28. **Radhakrishnan, S. K., and A. L. Gartel.** 2005. The PPAR-gamma agonist pioglitazone post-transcriptionally induces p21 in PC3 prostate cancer but not in other cell lines. Cell Cycle **4:**582–584.
29. **Rubin, M. A., N. R. Mucci, J. Figurski, A. Fecko, K. J. Pienta, and M. L. Day.** 2001. E-cadherin expression in prostate cancer: a broad survey using high-density tissue microarray technology. Hum. Pathol. **32:**690–697.
30. **Rubio, N., M. M. Villacampa, N. El Hilali, and J. Blanco.** 2000. Metastatic burden in nude mice organs measured using prostate tumor PC-3 cells expressing the luciferase gene as a quantifiable tumor cell marker. Prostate **44:**133–143.
31. **Sarruf, D. A., I. Iankova, A. Abella, S. Assou, S. Miard, and L. Fajas.** 2005. Cyclin D3 promotes adipogenesis through activation of peroxisome proliferator-activated receptor gamma. Mol. Cell. Biol. **25:**9985–9995.
32. **Segawa, Y., R. Yoshimura, T. Hase, T. Nakatani, S. Wada, Y. Kawahito, T. Kishimoto, and H. Sano.** 2002. Expression of peroxisome proliferator-activated receptor (PPAR) in human prostate cancer. Prostate **51:**108–116.
33. **Seligson, D. B., S. Horvath, T. Shi, H. Yu, S. Tze, M. Grunstein, and S. K. Kurdistani.** 2005. Global histone modification patterns predict risk of prostate cancer recurrence. Nature **435:**1262–1266.
34. **Shappell, S. B., R. A. Gupta, S. Manning, R. Whitehead, W. E. Boeglin, C. Schneider, T. Case, J. Price, G. S. Jack, T. M. Wheeler, R. J. Matusik, A. R. Brash, and R. N. Dubois.** 2001. 15S-Hydroxyeicosatetraenoic acid activates peroxisome proliferator-activated receptor gamma and inhibits proliferation in PC3 prostate carcinoma cells. Cancer Res. **61:**497–503.
35. **Smith, M. R., J. Manola, D. S. Kaufman, D. George, W. K. Oh, E. Mueller, S. Slovin, B. Spiegelman, E. Small, and P. W. Kantoff.** 2004. Rosiglitazone versus placebo for men with prostate carcinoma and a rising serum prostate-specific antigen level after radical prostatectomy and/or radiation therapy. Cancer **101:**1569–1574.
36. **Umbas, R., W. B. Isaacs, P. P. Bringuier, H. E. Schaafsma, H. F. Karthaus, G. O. Oosterhof, F. M. Debruyne, and J. A. Schalken.** 1994. Decreased E-cadherin expression is associated with poor prognosis in patients with prostate cancer. Cancer Res. **54:**3929–3933.
37. **Umbas, R., J. A. Schalken, T. W. Aalders, B. S. Carter, H. F. Karthaus, H. E. Schaafsma, F. M. Debruyne, and W. B. Isaacs.** 1992. Expression of the cellular adhesion molecule E-cadherin is reduced or absent in high-grade prostate cancer. Cancer Res. **52:**5104–5109.
38. **Wang, C., M. Fu, M. D'Amico, C. Albanese, J.-N. Zhou, M. Brownlee, M. P. Lisanti, V. K. Chatterjee, M. A. Lazar, and R. G. Pestell.** 2001. Inhibition of cellular proliferation through IκB kinase-independent and peroxisome proliferator-activated receptor gamma-dependent repression of cyclin D1. Mol. Cell. Biol. **21:**3057–3070.